

Phase Boundary for Flow-Induced Textures in $^3\text{He-A}$

D. M. Bates, S. N. Ytterboe, C. M. Gould, and H. M. Bozler

Department of Physics, University of Southern California, Los Angeles, California 90089

(Received 14 May 1984)

Texture transitions in superfluid $^3\text{He-A}$ are produced by a moving bellows system controlling mass flow. These texture changes are caused by the competition of magnetic, flow, and gradient energies. We have located the boundary of a region of stability with $\vec{v}_s \parallel \hat{l} \parallel \vec{H}$. This boundary may be related to theoretical predictions of a transition to helical textures, but there is substantial disagreement with the theory over the maximum magnitude of the superfluid velocity in what we interpret as uniform textures.

PACS numbers: 67.50.Fi, 43.35.+d, 47.20.+m

Textures in superfluid ^3He are a striking manifestation of the symmetry of the order parameter. To date, however, only a few relatively simple textures have been studied. We report here the first measurements on nontrivial dynamic textures in the A phase which are produced in a controlled fashion and which exhibit great sensitivity to the effect of superfluid flow. We have located a boundary between the uniform texture and a complex texture by varying the magnetic field while maintaining a constant mass flow.

The texture of superfluid $^3\text{He-A}$ results from the competition between several nonlinear energies that can be varied by changing the applied magnetic field H and the velocity of the superfluid v_s , as well as the temperature. These energies can be written in terms of the complex order parameter¹ consisting of an orbital unit vector \hat{l} and a spin-space unit vector \hat{d} . The free energy in the A phase^{2,3} is composed of a dipole energy F_D , a magnetic energy F_H , a flow energy F_v , and a gradient term F_{grad} involving bending of the order-parameter vectors l and d :

$$\begin{aligned} F &= F_D + F_H + F_v + F_{\text{grad}}, \quad F_D = -\lambda_D (\hat{l} \cdot \hat{d})^2, \quad F_H = \lambda_H (\hat{d} \cdot \vec{H})^2, \\ F_v &= \frac{1}{2} \rho_s v_s^2 - \frac{1}{2} \rho_0 (\hat{l} \cdot \vec{v}_s)^2 + c (\vec{v}_s \cdot \vec{\nabla} \times \hat{l}) - c_0 (\vec{v}_s \cdot \hat{l}) (\hat{l} \cdot \vec{\nabla} \times \hat{l}), \\ F_{\text{grad}} &= \frac{1}{2} K_s (\vec{\nabla} \cdot \hat{l})^2 + \frac{1}{2} K_l (\hat{l} \cdot \vec{\nabla} \times \hat{l})^2 + \frac{1}{2} K_b (\hat{l} \times \vec{\nabla} \times \hat{l})^2 + \frac{1}{2} K_1 [(\hat{l} \cdot \vec{\nabla}) \hat{d}]^2 + \frac{1}{2} K_2 [(\hat{l} \times \vec{\nabla}) \hat{d}]^2. \end{aligned} \quad (1)$$

For small relative flow velocities in the absence of other external forces, the anisotropy of the superfluid density causes the \hat{l} vector to line up with the flow as indicated in the second term of F_v , resulting in a uniform texture state with $\hat{l} \parallel \hat{d} \parallel \vec{v}_s$. In our experimental geometry, the measurements take place in a uniform tube, and thus we expect that the resulting textures are uniform in the plane perpendicular to the axis. For this reason, the third term in F_v will not contribute as long as \vec{v}_s remains parallel to the mass flow. The uniform texture is expected⁴ to become unstable at high velocities because of the c_0 term in the free energy, which tends to align $\vec{\nabla} \times \hat{l}$ with v_s . The presence of a magnetic field parallel to \vec{v}_s further destabilizes the uniform texture. Several theoretical studies of these energies have predicted a transition to a helical texture state when the magnetic field is increased.⁵ The helical texture is a screwlike distortion of \hat{l} and \hat{d} having a velocity-dependent pitch typically on the order of 10–100 μm . The opening angle of \hat{l} from the flow direction χ is predicted to increase from zero above a critical field H_c . An earlier experiment by Kleinberg⁶ observed a textural transition

by means of heat flow, but could not deduce a phase diagram. Other experiments^{7,8} have looked for transitions in large magnetic fields (> 100 G) where initially $v_s \perp \hat{l} \parallel \hat{d}$.

We have developed a flow cell⁹ which creates a constant driven mass flow (Fig. 1). A driven mass flow has the advantage that the flow can be well controlled and is independent of minor dissipation caused by textural changes in the fluid. The flow is created by use of a ^4He -filled bellows to drive a matched pair of ^3He -filled bellows which force fluid through a superleak consisting of 830 000 glass capillaries with 2- μm diameters while conserving the total ^3He volume. Constant superfluid flow velocities are obtained by use of a heated "bomb" to drive the ^4He bellows linearized with feedback from a mutual-inductance position detector. We can impose constant mass flows for several minutes at a time. The position of the bellows far from the experimental region insures that the mass flow at the experiment is superflow. There is certainly normal-fluid motion at both moving surfaces, but on one side the superleak blocks normal flow, and

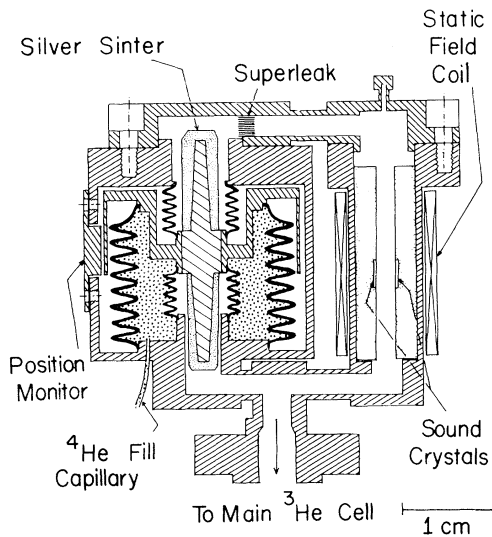


FIG. 1. Schematic representation of the flow cell. The ^3He bellows have an effective driving area of 0.77 cm^2 . The flow channel is formed by a removable epoxy insert containing the sound crystals. Rectangular channels with cross-sectional areas of 0.054 and 0.028 cm^2 have been used. The crystal spacing d for these two channels was 3.05 and 1.35 mm , respectively.

on the other, the imposition of our main liquid reservoir dilutes v_n to a negligible level.

The average orientation of the \hat{l} vector is detected by use of 30.8-MHz zero sound propagating across a rectangular flow channel positioned about 3 cm

from the superleak. The attenuation of zero sound is highly anisotropic in the A phase.¹⁰ For $T/T_c < 0.98$ and at 30.8 MHz the attenuation is less when sound propagates perpendicular rather than parallel to \hat{l} . In separate experiments we measured the sound attenuation anisotropy by slowly rotating the magnetic field in planes both perpendicular to and including the flow axis. Although this procedure leaves an ambiguity in the direction of \hat{l} , we were able to estimate the coefficients in the sound absorption, which has the form

$$\alpha - \alpha_c = A \sin^4 \theta + B \cos^4 \theta + 2C \sin^2 \theta \cos^2 \theta, \quad (2)$$

where θ is the angle between \hat{l} and the sound propagation vector \hat{q} . In the flow experiments, $\hat{q} \perp \vec{v}_s \parallel \vec{H}$ which is applied along the flow channel axis.

Figure 2 illustrates some typical behavior of the flow cell and indicates several important features of the experiment. S_{\perp} and S_{\parallel} represent the maximum and minimum sound levels observed at this particular temperature. With reference to Eq. (2), S_{\perp} can be used to estimate A , and S_{\parallel} measures some combination of A , B , and C , but is dominated by B . Before either flow or field is applied we observe large fluctuations of the sound signal. These fluctuations are strong evidence that the texture in this state is in fact fairly uniform on a large length scale. The texture responds to any residual forces caused by heat flow, fluctuating in direction on a time scale of a second. The application of a

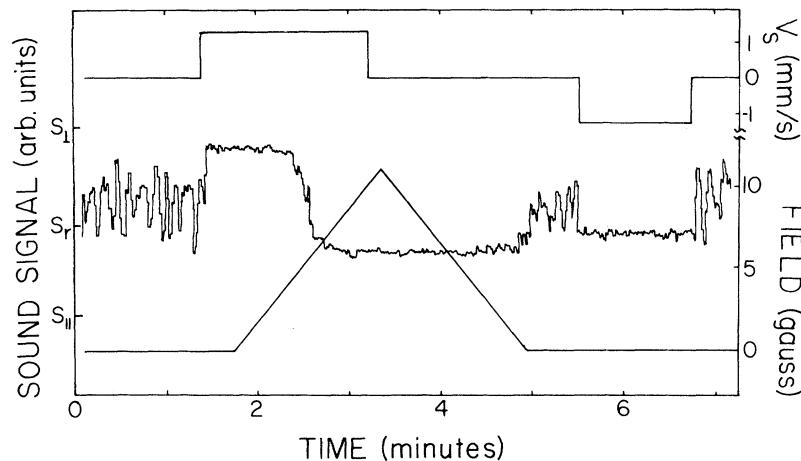


FIG. 2. Trace at $T=0.96T_c$ showing typical behavior of the superfluid when subjected to flow and field. Positive velocities are those in which the flow is towards the superleak. S_{\perp} corresponds to an attenuation of 1.7 cm^{-1} , S_{\parallel} corresponds to an attenuation of 11.0 cm^{-1} , and S_r is the sound signal level calculated for a completely random texture as described in the text. The first region has both flow and field at zero. At about 1.5 m the flow is started; subsequently the magnetic field is ramped. After the flow stops there is still enough field applied to suppress the oscillations which return when H approaches zero. The negative velocity pulse starting at about 5.5 m fails to produce the aligned texture expected.

constant-velocity bellows stroke (piston moving down) immediately suppresses these oscillations and brings the sound level up to near its maximum value, indicating that the \hat{l} texture is both uniform and aligned with the flow, and hence perpendicular to \hat{q} . The aligned state becomes unstable as an applied magnetic field is increased.

The last section of the experimental trace shows a quite surprising effect. When the bellows stroke is reversed (piston moves up), the sound does not reach the level associated with the aligned, uniform texture. Instead, we see a steady but smaller signal level. The sound signal measures the spatial average of the attenuation and thus the signature of the low constant signal is likely due to a complex texture forming between the sound crystals. For comparison, we have shown on Fig. 2 the expected sound level, S_r , for the case where \hat{l} varies randomly in space with zero mean. The most surprising aspect of this result is that this texture forms within a few seconds after the flow has started. We believe that this effect is due to the generation of unstable textures that are possibly created at the outlet of the superleak.

In order to determine the boundary of the uniform texture region (i.e., measure H_c vs v_s), we fit the sound signal to a simple function taken from the theory for helical textures. We assumed that for fields near the transition the opening angle χ for the \hat{l} helix will follow a field dependence $\sin^2\chi = b(H - H_c)$. Combining this with the form for the absorption anisotropy, computing the spatial average, and using $h = H - H_c$, we obtain

$$S = S_0 \exp \left\{ \left[-\frac{1}{2}(C - 2A)bh - \frac{3}{8}(A + B - C)b^2h^2 \right] d \right\} \quad (3)$$

for the sound signal S as H is increased beyond H_c . A , B , and C are the coefficients in Eq. (2), d is the crystal spacing, and b is a measure of the rate at which the helix opening angle increases with magnetic field. S_0 is the sound signal level before the transition. We first fitted the data by allowing b to vary. Since its effect is not orthogonal to S_0 and H_c it caused excess scatter in H_c . We did, however, find that b decreases with increasing v_s , in qualitative agreement with theoretical expectations, but the velocity scale would have to be increased by a factor of 4–5 in the theory to obtain agreement. Fixing b as a function of v_s , we then fitted the data with only S_0 and H_c as free parameters.

The resulting phase boundaries at 28.8 bars and three temperatures are plotted in Fig. 3(a)–(c). Only traces in which the sound level indicated a uniformly aligned starting texture were used in the

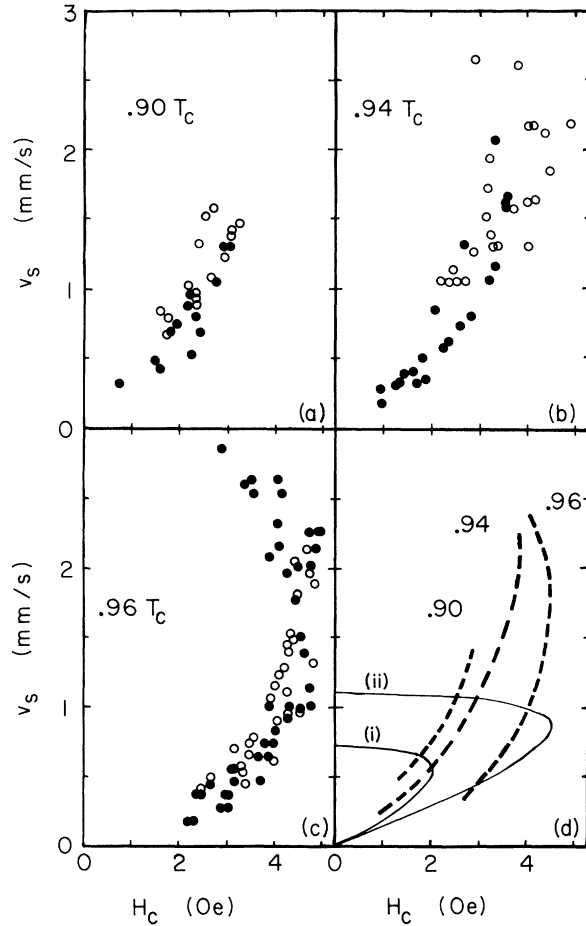


FIG. 3. Results for the phase boundary for the uniform texture region at $P=28.8$ bars. (a)–(c) Data taken at three temperatures in two different flow channels, with cross-sectional areas represented by circles (0.028 cm^2) and filled circles (0.054 cm^2). H_c is determined by fitting sound traces to Eq. (2). Smoothed data is shown for all three temperatures in (d). The solid curves in (d) are results of theoretical calculations for the boundary as a function of temperature. Curve (i) is calculated for $0.94 T_c$ with the weak coupling values of the free-energy coefficients. Curve (ii) is for one parameter increased by 10% as described in the text.

phase-boundary plots. The superfluid velocity v_s is derived from the bellows velocity, known geometrical factors, and $\rho_{s\parallel}$, the parallel component of the superfluid density tensor.¹¹ Some offset in the velocity is due to residual thermal current ($\approx 10^{-10} \text{ W}$). The dashed lines in Fig. 3(d) show the same data as in Fig. 3(a)–(c) after smoothing. Qualitatively, the transitions resemble the predictions of the helical texture theories.⁵ In particular, the experimentally determined boundary of the uniform texture has a critical field of similar magnitude as the predictions. Also we see that experimentally,

the region of stability shrinks at lower temperatures, as expected when the temperature dependence of the free energy is estimated.^{5,12} However, the uniform texture region appears to be stable for much higher velocities than predicted as we can see by comparing the results with curve (i) in Fig. 3(d) derived from the helical texture theory. Kleinberg⁶ also reported transitions at fields ranging from 0.5 to 5 G, but v_s was not accurately known.

We have considered several possibilities for the large quantitative discrepancy between the calculated and measured uniform texture regions. First is the question of whether the estimated values for parameters in the free energy are correct. The most important of these parameters are c_0 , K_b , and ρ_0 . The region of stability is indeed *very* sensitive to the actual values. For example, curve (ii) in Fig. 3(d) shows the effect of increasing the coefficient K_b by 10%, keeping all the other coefficients unchanged. Despite this sensitivity, however, we have not as yet found a way to fit the whole curve.

Another possibility is that we simply missed the "top" of the stable region because the expected angle of inclination χ at velocities above this region is small. We attempted to detect the upper bound of the uniform region by taking alternative paths in the H - \vec{v}_s plane by starting with a small constant velocity below the predicted upper limit of the uniform region along with a field of about $\frac{1}{2}H_c$, followed by increasing \vec{v}_s . These attempts failed to reveal a transition. Finally we must consider that there is some other mechanism that stabilizes the uniform texture at high flow rates. In future experiments we plan to explore texture transitions with differential pressure measurements and spin resonance.

We wish to thank K. Maki for helpful discus-

sions. This work was supported by the National Science Foundation through Grants No. DMR82-00661 and No. DMR82-08760. One of us (C.M.G.) is a recipient of an Alfred P. Sloan Research Fellowship.

¹A. J. Leggett, *Rev. Mod. Phys.* **47**, 331 (1975).

²M. C. Cross, *J. Low Temp. Phys.* **21**, 525 (1975).

³A. L. Fetter, *Phys. Rev. B* **20**, 303 (1979).

⁴P. Bhattacharyya, T.-L. Ho, and N. D. Mermin, *Phys. Rev. Lett.* **39**, 1290 (1977); M. C. Cross and M. Liu, *J. Phys. C* **11**, 1795 (1978).

⁵D. Vollhardt, Y. R. Lin-Liu, and K. Maki, *J. Low Temp. Phys.* **37**, 627 (1979); Y. R. Lin-Liu, D. Vollhardt, and K. Maki, *Phys. Rev. B* **20**, 159 (1979); A. L. Fetter and M. R. Williams, *Phys. Rev. B* **23**, 2102 (1981); and references cited therein.

⁶R. L. Kleinberg, *Phys. Rev. Lett.* **42**, 182 (1979).

⁷M. A. Paalanen and D. D. Osheroff, *Phys. Rev. Lett.* **45**, 362 (1980).

⁸E. B. Flint, R. M. Mueller, and E. D. Adams, *J. Low Temp. Phys.* **33**, 43 (1978).

⁹A description of the experimental techniques and preliminary data appear in D. M. Bates, C. M. Gould, and H. M. Bozler, in *Quantum Fluids and Solids—1983*, edited by E. D. Adams and G. G. Ihas, AIP Conference Proceedings No. 103 (American Institute of Physics, New York, 1983), p. 282–287.

¹⁰P. Wölfle, *Phys. Rev. Lett.* **30**, 1169 (1973), and in *Progress in Low Temperature Physics*, edited by D. F. Brewer (North-Holland, Amsterdam, 1978), Vol. 7A; J. Serene, Ph.D. thesis, Cornell University, 1973 (unpublished); D. N. Paulson, M. Krusius, and J. C. Wheatley, *J. Low Temp. Phys.* **26**, 73 (1977).

¹¹We used the values $\rho_{s\parallel}/\rho = 0.013, 0.020, 0.034$ for $T/T_c = 0.96, 0.94, 0.90$, respectively; J. E. Berthold, R. W. Giannetta, E. N. Smith, and J. D. Reppy, *Phys. Rev. Lett.* **37**, 1138 (1976).

¹²K. Maki and P. Kumar, *Phys. Rev. B* **17**, 1088 (1978).